CellPress

Cancer Cell
Article

Acetylation of Snail Modulates the Cytokinome of Cancer Cells to Enhance the Recruitment of Macrophages

Dennis Shin-Shian Hsu,[1] Hsiao-Jung Wang,[1] Shyh-Kuan Tai,[7] Chun-Hung Chou,[1] Chia-Hsin Hsieh,[2] Po-Hsien Chiu,[1] Nien-Jung Chen,[3,5] and Muh-Hwa Yang[1,2,4,5,6,8,*]

[1]Institute of Clinical Medicine, National Yang-Ming University, Taipei 11221, Taiwan
[2]Institute of Biotechnology in Medicine, National Yang-Ming University, Taipei 11221, Taiwan
[3]Institute of Microbiology and Immunology, National Yang-Ming University, Taipei 11221, Taiwan
[4]Genome Research Center, National Yang-Ming University, Taipei 11221, Taiwan
[5]Immunity and Inflammation Research Center, National Yang-Ming University, Taipei 11221, Taiwan
[6]Division of Hematology and Oncology, Department of Medicine, Taipei Veterans General Hospital, Taipei 11217, Taiwan
[7]Department of Otolaryngology, Taipei Veterans General Hospital, Taipei 11217, Taiwan
[8]Genomics Research Center, Academia Sinica, Taipei 11529, Taiwan
*Correspondence: mhyang2@vghtpe.gov.tw
http://dx.doi.org/10.1016/j.ccell.2014.09.002

SUMMARY

Snail is primarily known as a transcriptional repressor that induces epithelial-mesenchymal transition by suppressing adherent proteins. Emerging evidence suggests that Snail can act as an activator; however, the mechanism and biological significance are unclear. Here, we found that CREB-binding protein (CBP) is the critical factor in Snail-mediated target gene transactivation. CBP interacts with Snail and acetylates Snail at lysine 146 and lysine 187, which prevents the repressor complex formation. We further identified several Snail-activated targets, including TNF-α, which is also the upstream signal for Snail acetylation, and CCL2 and CCL5, which promote the recruitment of tumor-associated macrophages. Here, we present our results on the mechanism by which Snail induces target gene transactivation to remodel the tumor microenvironment.

INTRODUCTION

For tumors to metastasize, the cancer cells must gain enhanced migratory and tumor-initiating capacity, and the tumor microenvironment must be remodeled. During the metastatic process, the epithelial-mesenchymal transition (EMT) is the crucial mechanism by which cancer cells are reprogrammed to possess migratory and tumor-initiating capacity (Mani et al., 2008; De Craene and Berx, 2013). In addition to the canonical effects of EMT, increasing studies indicate that EMT has pleiotropic roles in cancer metastasis, including overriding oncogene-induced senescence (Ansieau et al., 2008), promoting invadopodia formation (Eckert et al., 2011), facilitating single-cell movement (Yang et al., 2012), and directing symmetric cell division (Hwang et al., 2014). However, it is largely unknown whether the cancer cells undergoing EMT are able to modulate the tumor microenvironment and what the role of EMT is in the interplay between tumor and host cells.

The EMT regulator Snail is a zinc finger transcription factor that is largely a transcriptional repressor. In cancer metastasis, Snail induces EMT by repressing E-cadherin expression (Cano et al., 2000). Mechanistically, Snail represses *CDH1* transcription by recruiting corepressors to the *CDH1* promoter and by modifying the chromatin, thereby promoting transcriptional silencing. The reported corepressor complexes of Snail include HDAC1/HDAC2/Sin3A for histone deacetylation (Peinado et al., 2004),

Significance

The understanding of Snail as an activator is relatively limited, compared with the knowledge of Snail as a repressor. Here, we identify the mechanism that guides the activity of Snail through the acetylation of Snail. The "yin and yang" effect of Snail is, therefore, elucidated; "repressor Snail" inhibits adherent protein expression to promote the disaggregation and migration of epithelial cancer cells, whereas "activator Snail" induces mesenchymal proteins to complete EMT and cytokine expression to remodel the tumor microenvironment. The paracrine effect of cells undergoing EMT has been highlighted, explaining the pivotal role of these stem-like cancer cells in host-cancer interplay.

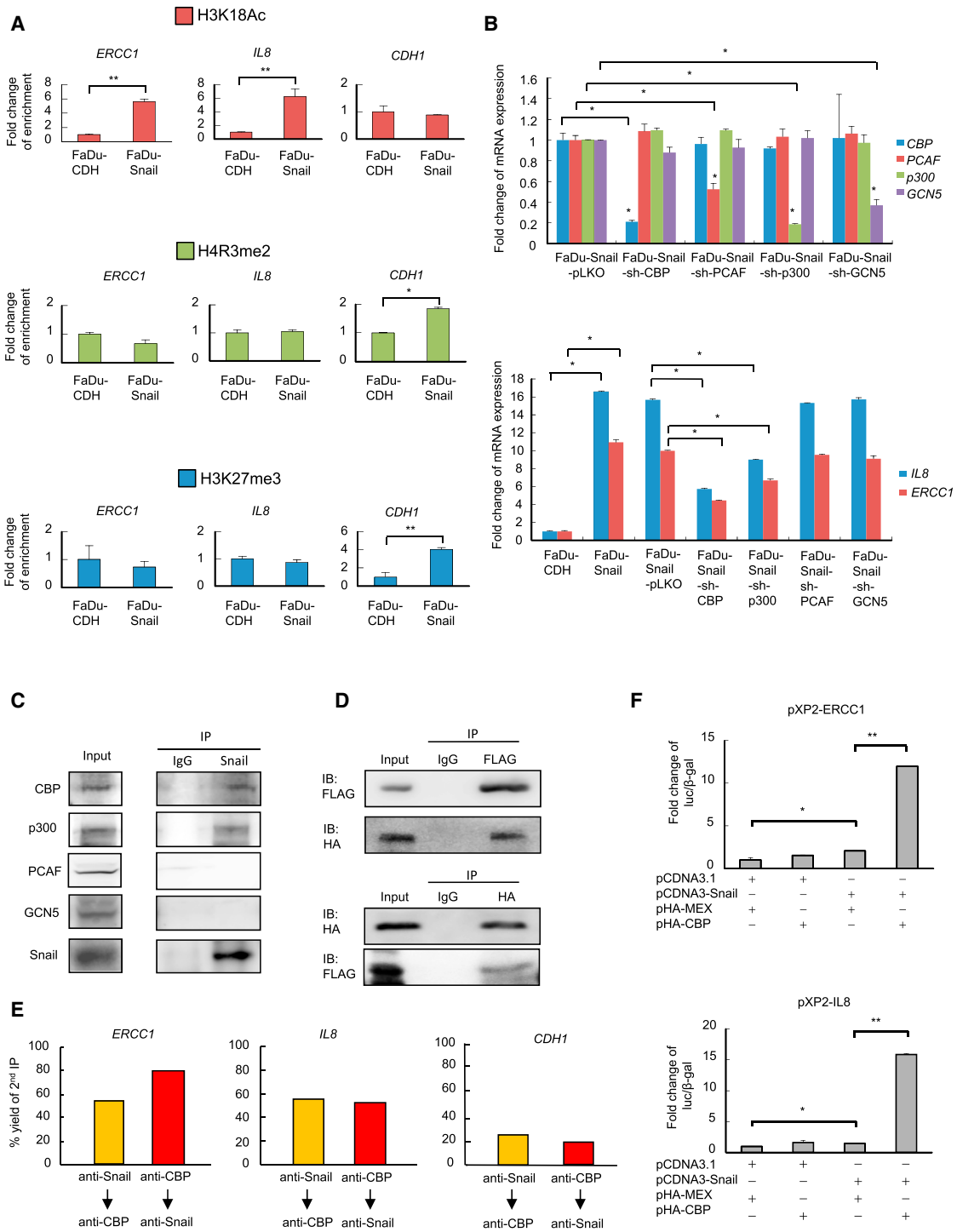

Figure 1. Snail Interacts with CBP/p300 to Activate Target Gene Transcription

(A) Quantitative ChIP for analyzing the enrichments of H3K18Ac (upper panel), H4R3me2 (middle panel), and H3K27me3 (lower panel) on the promoter of *ERCC1*, *IL8*, and *CDH1* in FaDu cells transfected with Snail (FaDu-Snail) or a control vector (FaDu-CDH). Data represent means ± SEM. *$p < 0.05$; **$p < 0.01$.

(B) Quantitative real-time PCR for confirming the knockdown efficiency of the acetyltransferases (*CBP*, *PCAF*, *p300*, and *GCN5*) and the expression of Snail target genes (*ERCC1* and *IL8*) in FaDu-CDH, FaDu-Snail, and FaDu-Snail receiving shRNA against different acetyltransferases or a control vector (pLKO). Data represent means ± SEM. *$p < 0.05$.

(C) Immunoprecipitation (IP)-western blot for detecting the association of endogenous Snail and different acetyltransferases in a head and neck cancer cell line OECM-1. IgG, immunoglobulin G.

(D) Immunoprecipitation-western blot for detecting the association between the ectopic CBP and Snail in 293T cells cotransfected with pHA-CBP and pFLAG-Snail. IB, immunoblot.

(legend continued on next page)

polycomb repressive complex for histone 3 lysine 27 trimethylation (H3K27me3) (Herranz et al., 2008), and PRMT5 for histone 4 arginine 3 dimethylation (H4R3me2) (Hou et al., 2008). Accumulating evidence suggests that Snail could be a transcriptional activator. Snail expression triggers euchromatin changes in certain mesenchymal genes, thereby inducing EMT (Wu et al., 2011; Javaid et al., 2013). In *Drosophila*, Snail potentiates activator-mediated target gene expression (Rembold et al., 2014). Snail directly activates the transcription of *ERCC1* and *IL8* (Hsu et al., 2010; Hwang et al., 2011) and cooperates with p65 to induce the expression of fibronectin 1 (Stanisavljevic et al., 2011). However, the mechanism and significance of Snail as an activator are unclear. In this study, we aim to identify the mechanism of Snail-induced target gene activation and its biological significance for cancer progression.

RESULTS

CBP/p300 Interacts with Snail and Promotes Transcriptional Activation of Snail Target Genes

The initial aim of this study was to investigate the mechanism of Snail-induced target gene transactivation. We hypothesized that histone marks surrounding the Snail-binding area of Snail-activated genes would differ from those surrounding Snail-repressed genes, resulting in the differential regulation of Snail target genes. To this end, *ERCC1* and *IL8* were used as model Snail-activated genes, and *CDH1* was a model Snail-repressed gene. Chromatin immunoprecipitation (ChIP) was performed in FaDu cells, a head and neck cancer cell line, which stably expressed either a Snail vector (FaDu-Snail) or a control vector (FaDu-CDH). The results showed that overexpression of Snail enhanced histone acetylation, including histone 3 lysine 4 acetylation (H3K4Ac), histone 3 lysine 14 acetylation (H3K14Ac), and histone 3 lysine 18 acetylation (H3K18Ac) on the promoters of *ERCC1* and *IL8*. This enrichment of histone acetylation was only observed on Snail-activated genes, not on *CDH1*. Conversely, the reported Snail-associated repressive marks on *CDH1*, specifically H3K27me3 and H4R3me2, were not enriched on Snail-activated genes (Figure 1A; Figure S1A available online). A similar change in these histone marks was observed when FaDu cells were treated with transforming growth factor beta (TGFβ), a known inducer of Snail expression and EMT (De Craene and Berx, 2013) (Figure S1B). We next sought to uncover the primary histone acetyltransferases (HATs) responsible for Snail-induced target gene expression. To this end, we knocked down different HATs in FaDu-Snail transfectants and observed the effect on the expression of Snail-activated target genes. Of the various HATs, knockdown of CREB-binding protein (CBP) or p300 attenuated Snail-induced target gene expression to the greatest extent (Figure 1B). Therefore, we hypothesized that Snail recruits CBP/p300 to the promoter of activated target genes as a coactivator. The coimmunoprecipitation experiment showed that Snail was physically associated with CBP/p300 (Figures 1C and 1D). Snail interacted with CBP through amino acids (aa) 60–90 (Figure S1C), and the CBP fragment aa 1101–1679, which contains HAT domain, was responsible for the CBP-Snail interaction (Figure S1D). Snail and CBP co-occupied the promoter of *ERCC1* and *IL8* but less frequently occupied the *CDH1* promoter (Figure 1E). CBP significantly augmented Snail-induced activation of target genes (Figure 1F). These results suggest that CBP/p300 interacts with Snail and that they co-occupy the promoters of target genes to induce transcriptional activation.

Snail Is Acetylated by CBP at Lysine 146 and Lysine 187

In addition to its role as a HAT (Berger, 2007), CBP/p300 has been shown to acetylate interacting proteins to modulate their function (Gu and Roeder, 1997; Ito et al., 2001). We investigated whether CBP/p300 acetylates Snail. The ectopic expression of CBP enriched Snail acetylation (Figure 2A). In Snail transfectants, the knockdown of CBP/p300, but no other HATs, reduced Snail acetylation (Figure 2B). Mass spectrometry analysis identified that lysine 146 and lysine 187 on the zinc finger domain of Snail were acetylated by CBP (Figure 2C), and these two residues were highly conserved across species (Figure 2D). In vitro acetylation assays confirmed the acetylation of lysine 146 and lysine 187 on Snail by a HAT (Figure 2E). Mutation of either site attenuated CBP-induced Snail acetylation, and mutations at both of these sites abrogated the acetylation (Figure 2F). A proximity ligation assay (PLA) provided additional evidence to support the acetylation of Snail by CBP (Figures S2A and S2B). To further confirm CBP-induced Snail acetylation, we generated antibodies to specifically recognize lysine 146- or lysine 187-acetylated Snail (Figure S2C). Knocking down CBP, but not other HATs, reduced lysine 146 or lysine 187 acetylation in the Snail transfectants, as recognized by the antibodies (Figure S2D). The expression of CBP increased Snail acetylation on lysine 146 and lysine 187, while mutation of either residue abrogated the acetylation (Figure 2G). These data suggest that Snail is a substrate for CBP-mediated acetylation.

Snail Acetylation Prevents the Assembly of the Repressor Complex and Stabilizes Snail without Affecting Its DNA-Binding Ability and Subcellular Localization

Next, we investigated the effect of Snail acetylation on Snail-mediated transcriptional activation. The inhibition of HAT activity partially abrogates the transactivation of Snail-mediated target genes (Figure S3A), suggesting that both the transcriptional activity potential and HAT activity of CBP contribute to Snail-induced target gene transcription. We further investigated whether CBP and the corepressors were present in the same complex. A coimmunoprecipitation experiment showed that CBP and the corepressor Ajuba were not present in the same complex (Figure 3A). Both an anti-CBP antibody and an anti-Sin3A antibody were able to pull down Snail. However,

(E) Sequential ChIP for analyzing the co-occupancy of Snail and CBP on the promoter of *ERCC1*, *IL8*, and *CDH1* in FaDu-Snail cells. Data represent yields of secondary immunoprecipitation.
(F) Luciferase (luc) reporter assay. The 293T cells were cotransfected with the reporter plasmid containing *ERCC1* (pXP2-ERCC1) or *IL8* (pXP2-IL8) promoter and different expression vectors as indicated. β-gal, β-galactosidase. Data represent means ± SEM. *$p < 0.05$; **$p < 0.01$.
See also Figure S1.

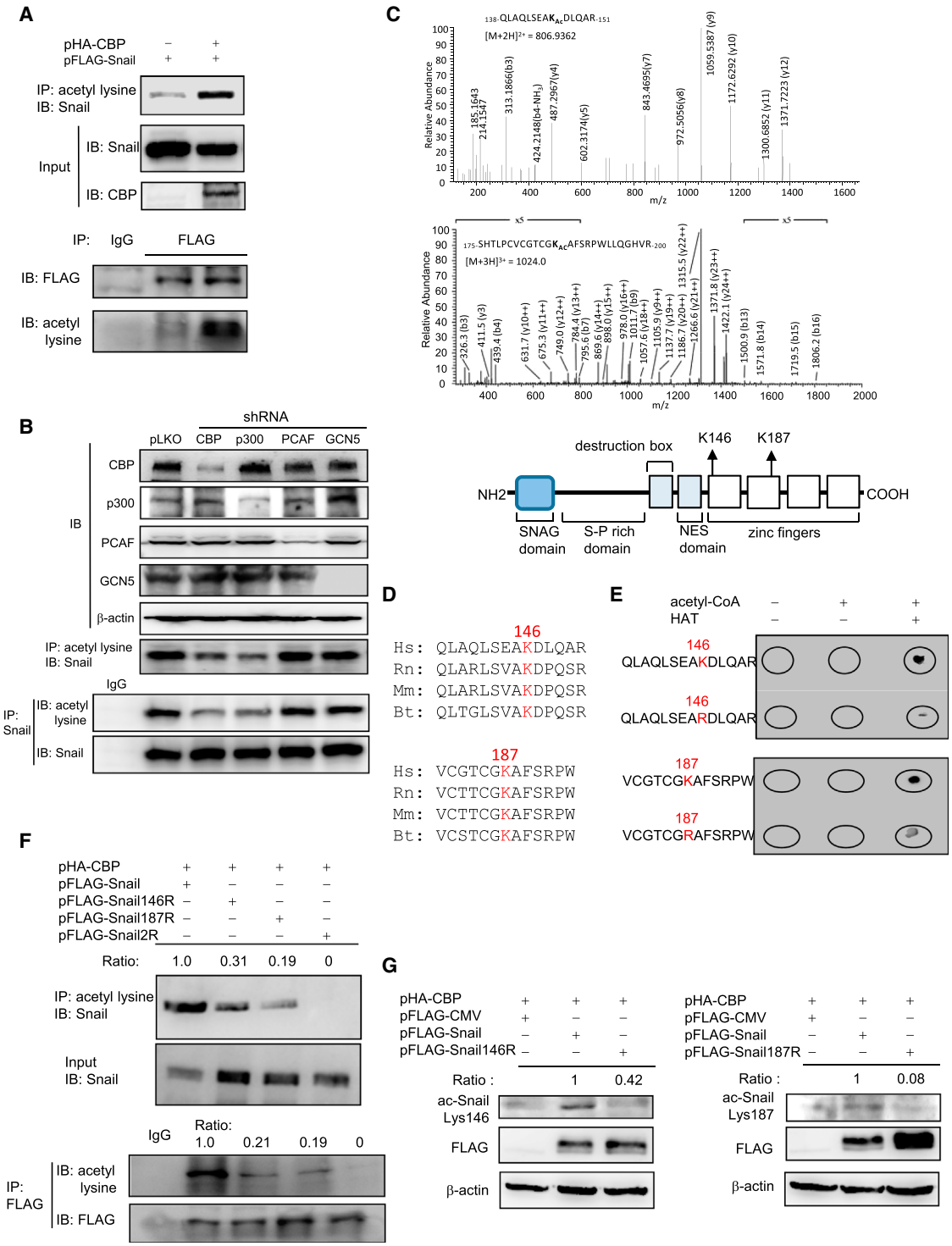

Figure 2. Snail Is Acetylated by CBP at Lysine 146 and Lysine 187

(A) Immunoprecipitation (IP)-western blot for analyzing the acetylated Snail in 293T cells transfected with pFLAG-Snail with/without cotransfection of pHA-CBP. IB, immunoblot.

(B) Immunoprecipitation-western blot for analyzing the acetylated Snail in FaDu-Snail transfectants receiving shRNA against different acetyltransferases or a control vector (pLKO). β-actin was a loading control for immunoblots.

(C) Upper panel: mass spectrometry for determining the acetylation sites of Snail by analyzing the purified Snail proteins from 293T cells cotransfected with GST-Snail and pHA-CBP. Lower panel: schematic representation of the acetylated sites on Snail.

(D) Alignment of Snail amino acids sequence among different species. Hs, *Homo sapiens*; Rn, Rattus norvegicus; Mm, *Mus musculus*; Bt, Bos taurus.

(legend continued on next page)

acetylated Snail was only present in the CBP-associated complex, and HDAC1 and HDAC2 were found in the Sin3A-containing complex (Figure 3B). Ectopic CBP inhibited the interaction between WT Snail and the corepressors (Ajuba, HDAC1, and HDAC2) but had no effect on the interaction between the nonacetylatable Snail mutant (Snail2R) and corepressors (Figure 3C). The corepressors Ajuba and Sin3A did not occupy the promoters of Snail-activated genes (Figure 3D). Furthermore, a greater enrichment of acetylated Snail was shown on the promoters of Snail-activated genes than on *CDH1* (Figure 3E). Because the HDAC1/HDAC2/Sin3A complex is critical for Snail-mediated target gene repression (Peinado et al., 2004), we wondered whether HDAC1/HDAC2 was able to deacetylate Snail to facilitate the formation of the repressor complex. Treatment with the HDAC inhibitor trichostatin (TSA), but not the SIRT1 inhibitor nicotinamide (NAM), enhanced Snail acetylation (Figure 3F). The knockdown of either HDAC1 or HDAC2 increased Snail acetylation (Figure 3G). HDAC1 deacetylates Snail at lysine 146, and HDAC2 deacetylates Snail at both lysine 146 and lysine 187 (Figure 3H).

Snail has been shown to activate *FN1* expression through cooperation with p65 (Stanisavljevic et al., 2011). To investigate whether Snail acetylation is involved in this event, we examined the expression of fibronectin in FaDu cells expressing Snail (FaDu-Snail) or the Snail2R mutant (FaDu-Snail2R). An upregulation of *FN1* was shown in FaDu-Snail, but not FaDu-Snail2R, transfectants compared with the control cells (Figure S3B). Acetylated Snail was associated with p65, while nonacetylatable Snail mutant did not interact with p65 (Figures S3C and S3D). Furthermore, p65, CBP, and Snail were present in the same complex (Figure S3E). The acetylated Snail and p65 co-occupied the promoter of *FN1* (Figure S3F), and Snail and p65 synergistically activated the *FN1* promoter (Figure S3G).

We next examined the impact of Snail acetylation on the stability, DNA-binding ability, and localization of Snail. GSK-3β can phosphorylate Snail and promotes its polyubiquitination and degradation (Zhou et al., 2004). Here, we show that the wild-type (WT) Snail is more stable than the nonacetylatable Snail2R mutant (Figures S3H and S3I). The acetylation of Snail by CBP reduced its phosphorylation; however, CBP showed no impact on either the phosphorylation or the acetylation of the Snail2R mutant (Figure S3J). Snail2R is more prone to be polyubiquitinated than WT Snail (Figure S3K). Inhibition of HAT activity by C646 increased the polyubiquitination of WT Snail. However, the polyubiquitination of Snail that has been mutated in its GSK3β phosphorylation site (Snail6SA; Zhou et al., 2004) was unaffected by C646 (Figure S3L). Snail acetylation affected neither the DNA-binding ability nor the subcellular localization of Snail (Figures S3M and S3N). Interestingly, the expression of Snail2R in FaDu cells only induced a partial EMT. Repression of the epithelial markers γ-catenin and E-cadherin was preserved in FaDu-Snail2R. However, less induction of the mesenchymal protein fibronectin was found in FaDu-Snail2R compared with FaDu-Snail (Figures S3O and S3P). Collectively, our data suggest that acetylated Snail is associated with coactivators, while nonacetylated Snail interacts with corepressors. Snail acetylation increases the stability of Snail without affecting its DNA-binding ability and subcellular localization.

TNF-α-IKKα Is Upstream of Snail Acetylation

Under tumor necrosis factor alpha (TNF-α) stimulation, CBP is phosphorylated by IκB kinase (IKK)α at serine 1382 and serine 1386 to increase its acetyltransferase activity (Huang et al., 2007). We investigated whether TNF-α can serve as an external stimulus for increasing Snail acetylation and activity through IKKα-CBP. First, we examined the impact of CBP phosphorylation on Snail acetylation and activity. Although both phosphomimetic CBP (EE-CBP) and unphosphorylatable CBP (AA-CBP) interacted with Snail (Figure 4A), EE-CBP had a higher ability to promote Snail acetylation compared with AA-CBP (Figure 4B). EE-CBP also augmented Snail-induced target gene transactivation more prominently than did AA-CBP (Figure 4C). Next, we investigated whether the TNF-α-IKKα axis is responsible for this effect. Exogenous TNF-α increased Snail acetylation in different types of cancer cells (Figure 4D). In FaDu cells, phosphorylated IKKα, phosphorylated CBP, and acetylated Snail were correspondingly increased on TNF-α stimulation (Figure 4E). Murine TNF-α induced Snail acetylation in mouse embryonic fibroblasts (MEFs) from IKKβ- or IKKγ-knockout (KO) mice but not in MEFs from IKKα-KO mice (Figure 4F). Compared with FaDu-control cells, TNF-α significantly upregulated *ERCC1* and *IL8* in FaDu-Snail but not in FaDu-Snail2R (Figure 4G). In the colon cancer cell line HCT15, inhibiting either TNF-α (with the TNF-α inhibitor TNFI or etanercept) or CBP activity (by C646) abrogated Snail-induced target gene expression (Figure 4H). These data suggest that the TNF-α-IKKα-CBP pathway increases Snail acetylation and activity.

TNFA, *CCL2*, and *CCL5* Are Target Genes Transactivated by Snail

We next investigated the global effect of Snail acetylation on target gene expression. A complementary DNA (cDNA) microarray showed that the expression profile was different between FaDu-Snail and FaDu-Snail2R (Figure 5A; Table S1). Among the differentially expressed genes, the immune response genes were the most prominent group (Figure 5B). There were other genes upregulated in FaDu-Snail but not in FaDu-Snail2R, including the mesenchymal genes, such as *FN1* (Figure S2F), *ZEB1*, and *THBS1* (Figure S4A). Here, we focused on cytokine genes because the immune response genes are the major

(E) In vitro acetylation assay. The biotin-labeled peptides containing the sequence surrounding Snail lysine 146 (upper panel) and lysine 187 (lower panel), or replaced lysine 146/187 with arginine, were incubated with HAT and acetyl Co-A and then analyzed by dot blot.
(F) Immunoprecipitation-western blot for analyzing the acetylated Snail in 293T cells cotransfected with pHA-CBP and a vector expressing WT Snail (pFLAG-Snail), Snail aa 146 Lys-to-Arg mutation (p-FLAGSnail146R), Snail aa 187 Lys-to-Arg mutation (pFLAG-Snail187R), and double mutation of Snail Lys146 and Lys187 (pFLAG-Snail2R).
(G) Western blot using the antibody specifically recognizing lysine-146-acetylated Snail (left panel) or lysine-187-acetylated Snail (right panel) in 293T cells cotransfected with pHA-CBP and a WT or the acetylation site-mutated Snail expression vector. β-actin was a loading control.
See also Figure S2.

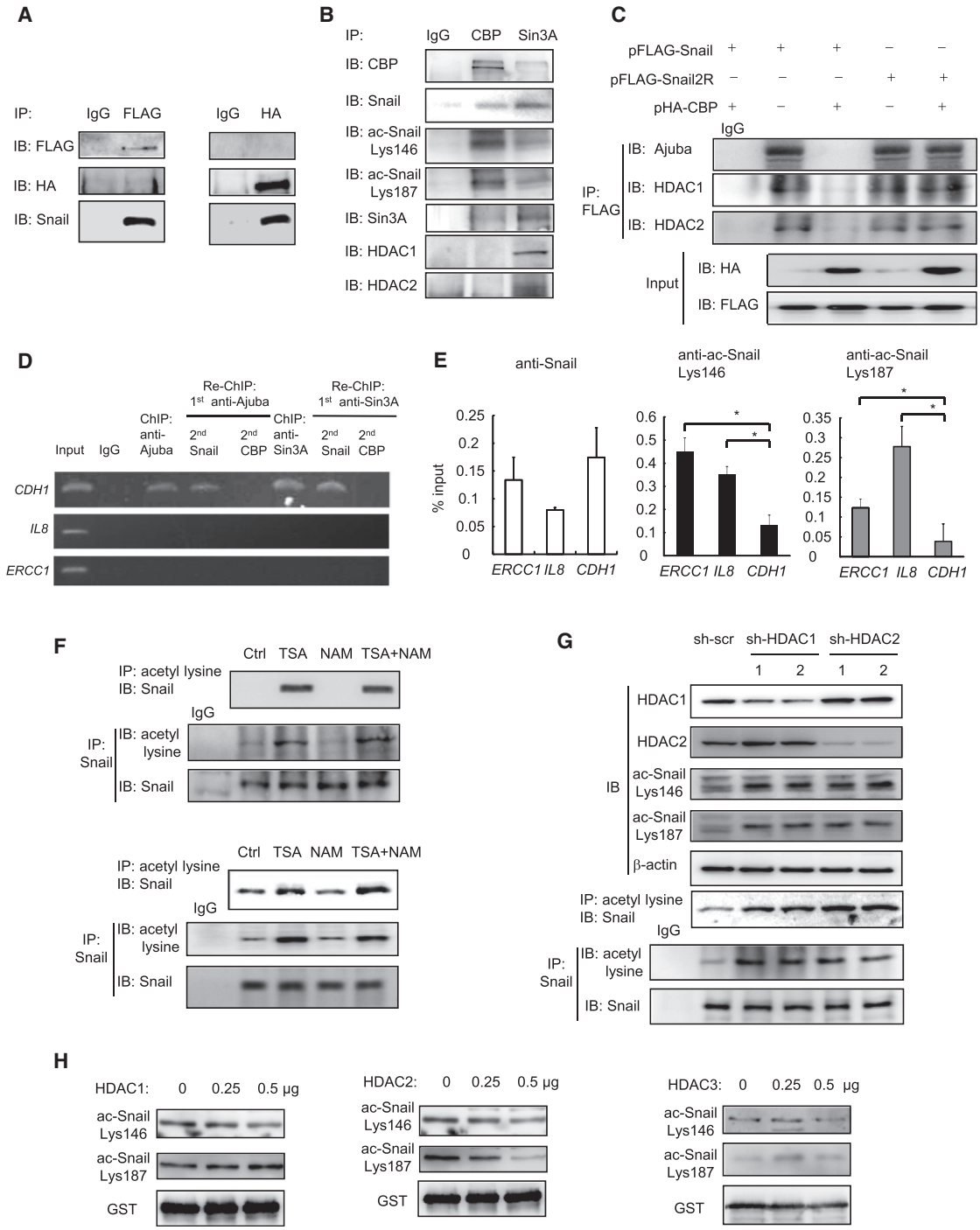

Figure 3. Acetylation of Snail Prevents the Assembly of the Snail Repressor Complex, and HDAC1/HDAC2 Deacetylates Snail

(A) Immunoprecipitation (IP)-western blot of 293T cells cotransfected with pHA-Ajuba, pFLAG-CBP, and pcDNA3-Snail. The protein lysates were immunoprecipitated and immunoblotted with indicated antibodies. IgG, immunoglobulin G; IB, immunoblot.

(B) Immunoprecipitation-western blot of FaDu cells. The lysates were immunoprecipitated and immunoblotted with the indicated antibodies.

(C) Immunoprecipitation-western blot of 293T cells stably transfected with WT Snail (pFLAG-Snail) or the non-acetylatable Snail mutant (pFLAG-Snail2R) with or without co-transfection of pHA-CBP. The lysates were immunoprecipitated and immunoblotted with the indicated antibodies.

(D) ChIP and sequential ChIP in FaDu cells. The protein-DNA was cross-linked and sequentially immunoprecipitated by one or two antibodies as indicated. The DNA fragments containing the Snail binding sites on the promoter of different genes (*CDH1*, *IL8*, and *ERCC1*) were amplified by PCR and analyzed by electrophoresis.

(legend continued on next page)

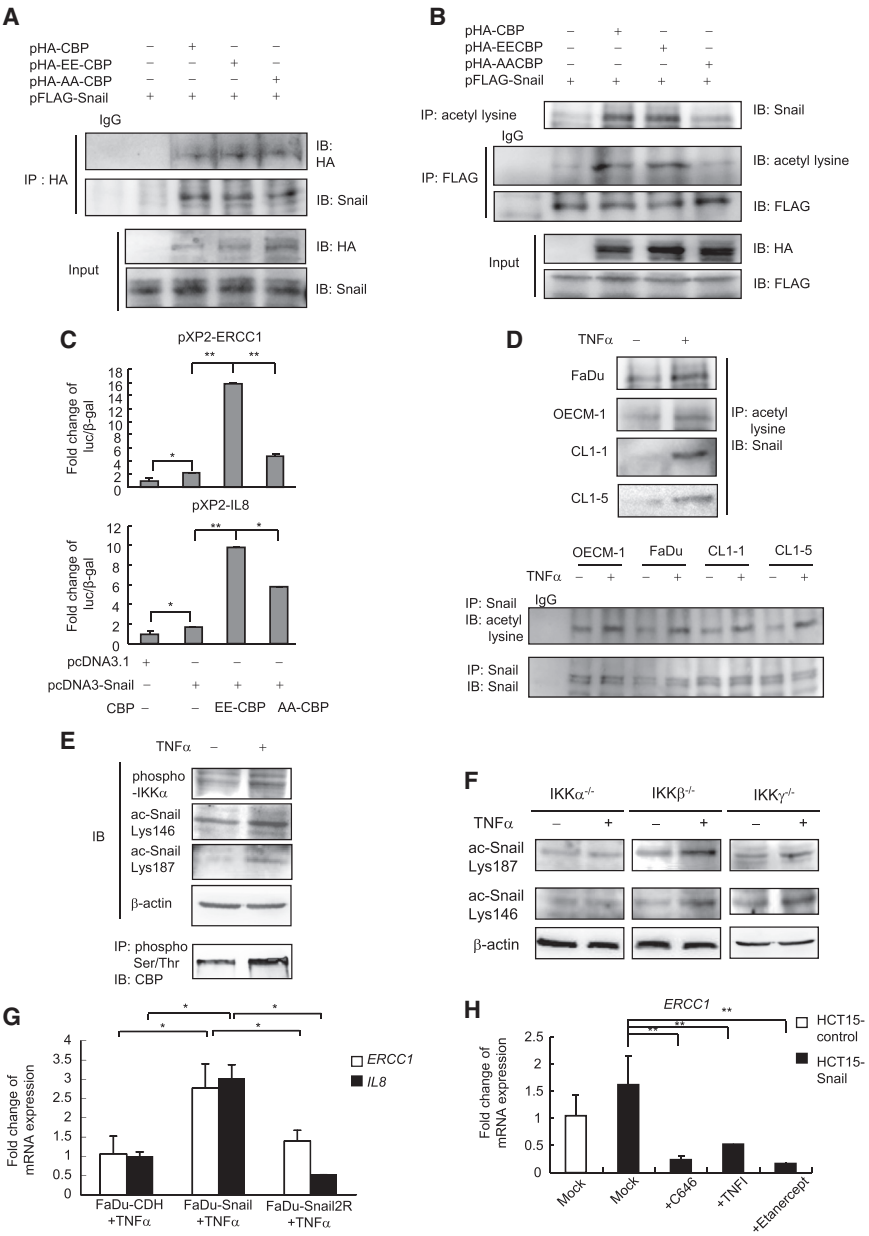

Figure 4. TNF-α-CBP Axis Promotes Snail Acetylation

(A) Immunoprecipitation (IP)-western blot for analyzing the interaction between Snail and WT CBP, phosphomimetic CBP (EE-CBP), or non-phosphorylatable CBP (AA-CBP). The 293T cells were cotransfected with WT Snail (pFLAG-Snail) and the indicated plasmids. IgG, immunoglobulin G. IB, immunoblot.

(B) Immunoprecipitation-western blot for analyzing acetylated Snail in 293T cells co-transfected with WT CBP/EECBP/AACBP and pFLAG-Snail.

(C) Luciferase reporter assay. The 293T cells were cotransfected with the promoter reporter construct (upper panel: pXP2-ERCC1; lower panel, pXP2-IL8) and different expression vectors as indicated. Data represent means ± SEM. *$p < 0.05$; **$p < 0.01$.

(D) Immunoprecipitation-western blot for analyzing the acetylated Snail in four cancer cell lines (FaDu, OECM-1, CL1-1, and CL1-5) treated with 20 ng/ml TNF-α for 8 hr or a vehicle control.

(E) Western blot for analyzing the phosphorylated IKKα and acetylated Snail and immunoprecipitation-western blot for detecting phosphorylated CBP in FaDu cells treated with 20 ng/ml TNF-α for 8 hr or a vehicle control. β-actin was a loading control for immunoblots.

(F) Western blot for detecting acetylated Snail in MEFs from IKKα$^{-/-}$, IKKβ$^{-/-}$, or IKKγ$^{-/-}$ mice treated with 20 ng/ml murine TNF-α for 8 hr or a vehicle control.

(G) Quantitative real-time PCR for analyzing the messenger RNA (mRNA) level of *ERCC1* and *IL8* in FaDu cells stably transfected with a WT Snail (FaDu-Snail)/non-acetylatable Snail mutant (FaDu-Snail2R) or an empty vector (FaDu-CDH) and treated with 20 ng/ml TNF-α for 8 hr. Data represent means ± SEM. *$p < 0.05$.

(H) Quantitative real-time PCR for analyzing the expression of *ERCC1* in HCT15-Snail versus HCT15-control treated with different inhibitors. C646 is a CBP/p300 inhibitor (6 μM for 8 hr). TNFI is a TNFR inhibitor (30 μM for 8 hr), and etanercept is a soluble receptor for neutralizing TNF-α (25 μg/ml for 8 hr). Data represent means ± SEM. **$p < 0.01$.

group of Snail-activated genes and the Snail-induced cytokine change has not yet been exhaustively investigated. We first investigated the paracrine effect of acetylated Snail-expressing cancer cells. The results showed that the conditioned medium from FaDu-Snail cells, but not from FaDu-Snail2R or FaDu-control cells, enhanced Snail acetylation (Figure 5C) and target gene

(E) Quantitative ChIP in FaDu cells. The protein-DNA was crosslinked and immunoprecipitated by an anti-Snail (left), anti-acetylated Snail lysine 146 (middle), or anti-acetylated Snail lysine 187 (right) antibody. The DNA fragments containing the Snail binding sites on the promoter of different genes (*CDH1*, *IL8*, and *ERCC1*) were amplified by quantitative PCR and presented as the percentage of input. Data represents means ± SEM. *$p < 0.05$.

(F) Immunoprecipitation-western blot for analyzing acetylated Snail in Snail-transfected 293T cells (upper) and FaDu-Snail cells (lower) treated with a vehicle control (Ctrl), a HDAC inhibitor TSA 5 nM for 8 hr, a SIRT1 inhibitor NAM 10 mM for 8 hr, or in combination.

(G) Immunoprecipitation-western blot for analyzing the acetylated Snail in Snail-transfected 293T cells receiving shRNA against HDAC1 or HDAC2. Each target was knocked down by two independent shRNA sequences. Transfection of the scrambled sequence (scr) was a control for shRNA experiment. The acetylated Snail is detected by immunoprecipitation-western blot or acetylated Snail-specific antibodies.

(H) In vitro deacetylation assay. The GST-Snail (purified from 293T cells cotransfected with pGST-Snail and pHA-CBP) was coincubated with indicated doses of HDAC1, HDAC2, or HDAC3 for 30 min then immunoblotted with the anti-acetylated Snail lysine 146 and anti-acetylated Snail lysine 187 antibodies. HDAC3 is a control for confirming the specific deacetylation effect of HDAC1/2 on Snail.

See also Figure S3.

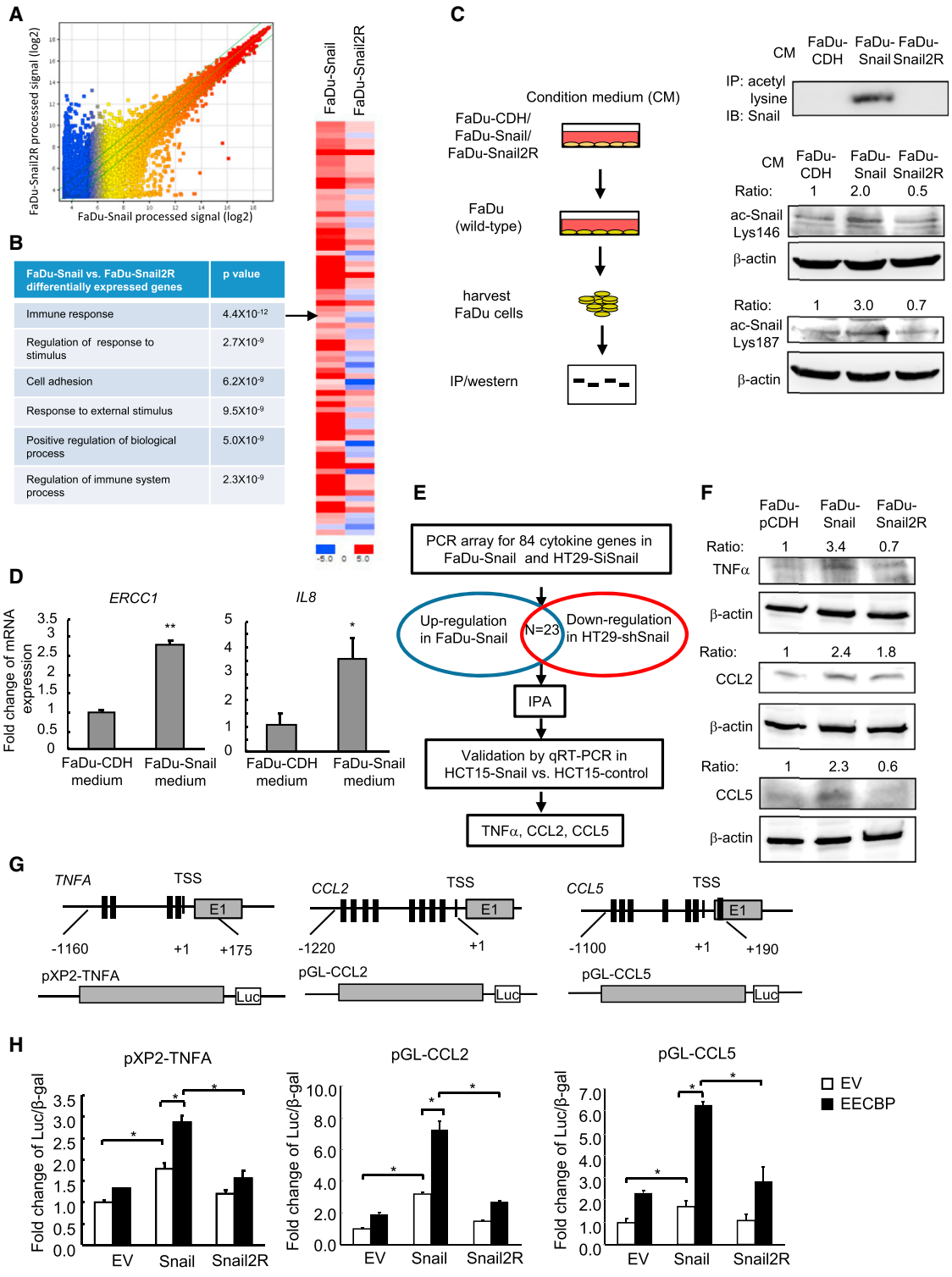

Figure 5. TNF-α, CCL2, and CCL5 Are Downstream Targets of Snail

(A) A scatterplot showing the results of the cDNA microarray in FaDu-Snail versus FaDu-Snail2R.

(B) Left: a table summarizing the results of the cDNA microarray data analyzed by gene ontology. Right: a heatmap showing the differentially expressed genes related to immune responses.

(C) Left: schema for representing the experiment procedure. Right: analyzing the acetylated in WT FaDu cells treated with the supernatant from FaDu-CDH, FaDu-Snail, or FaDu-Snail2R by immunoprecipitation (IP)-western blot (upper panel) or the acetylated-Snail specific antibodies (lower panel). The fold change of acetylated Snail was shown. CM, conditioned medium; IB, immunoblot.

(legend continued on next page)

expression in WT FaDu cells (Figure 5D). To determine the major cytokine genes regulated by Snail, a PCR array was performed in FaDu-Snail versus FaDu-control cells and HT-29 cells receiving small hairpin RNA (shRNA) against Snail or control. Ingenuity pathway analysis (IPA) was used to narrow down the target genes, and we validated the result in an independent cell line, HCT-15 (Figure 5E; Figures S4B and S4C). A number of cytokine genes were induced by Snail in the PCR array analysis (Table S2). The expression and secretion of interleukin-6, an inflammatory cytokine that plays an important role in cancer progression (Guo et al., 2012) and has been shown to be upregulated by Snail (Lyons et al., 2008), was increased in FaDu-Snail but not in FaDu-Snail2R (Figure S4D). Here, we focused on TNF-α, CCL2, and CCL5 because they are located in the center of the signaling network from IPA analysis (Figure S4B), suggesting their importance in the Snail-modulated cytokinome. Furthermore, TNF-α is critical for maintaining/amplifying Snail acetylation signal through a positive feedback loop. Ectopic Snail, but not Snail2R, increased the expression of CCL2, CCL5, and TNF-α (Figure 5F) and enhanced their secretion (Figure S4E). Knocking down Snail repressed the expression of CCL2, CCL5, and TNF-α (Figures S4F–S4I). Transfection of WT Snail, but not Snail2R, increased the promoter activity of *CCL2*, *CCL5*, and *TNFA*, and the coexpression of a phosphomimetic CBP further augmented this effect (Figures 5G and 5H). A ChIP assay confirmed the direct binding of Snail to the promoters of these genes (Figure S4J). Mutation of the Snail acetylation sites (Snail2R) or neutralization of TNF-α by etanercept abrogated the expression of Snail target genes (Figure S4K).

We further examined whether the expression of *TNFA*/*CCL2*/*CCL5* is Snail dependent because they are known targets of the TNF-α-NFκB pathway (Goldfeld et al., 1990; Ueda et al., 1997; Wickremasinghe et al., 2004). Under TNF-α treatment, the suppression of NFκB activity attenuated the expression of *CCND1*, a known target gene of NFκB (Guttridge et al., 1999), in both FaDu-Snail and FaDu-control cells (Figure S4L). However, inhibiting NFκB activity only partially abrogated the expression of *CCL2*, *CCL5*, and *IL8* in FaDu-Snail cells (Figure S4M). Knocking down endogenous Snail reduced the induction of *TNFA*, *CCL2*, and *CCL5* expression by TNF-α (Figure S4N). These results suggest that *CCL2*, *CCL5*, and *TNFA* are target genes that are activated by acetylated Snail. TNF-α and Snail form a positive feedback loop that amplifies the signal.

Snail Acetylation Promotes the Recruitment of Macrophages and Facilitates Tumor Progression

Next, we investigated the functional impact of Snail acetylation in cancer cells. Interestingly, we found that many Snail target genes are chemoattractants for tumor-associated macrophages (TAMs). CCL2 and CCL5 promote the recruitment of TAMs (Azenshtein et al., 2002; Qian et al., 2011). Interleukin-8 (IL8) is the ligand of CXCR1 and CXCR2 (Loetscher et al., 1994), which are highly expressed on the surface of M2 macrophages (Mantovani et al., 2002), and TAMs are considered to have an M2-like phenotype (Biswas and Mantovani, 2010). Therefore, we examined whether Snail-induced chemokine secretion is critical for this effect. The results revealed that the overexpression of Snail, but not of Snail2R, increased the chemoattraction of FaDu cells to $CD14^+$ monocytes (Figures 6A and 6B). The neutralization of Snail-induced cytokines (CCL2, CCL5, or IL8) attenuated monocyte migration (Figure 6C). An increased rapid recruitment of $CD14^+$ human monocytes to the lungs was observed in mice that were coinjected with FaDu-Snail cells compared with mice that were coinjected with FaDu-Snail2R/FaDu-control cells (Figure 6D). The conditioned medium from FaDu-Snail cells, but not from FaDu-Snail2R/FaDu-control cells, increased the expression of surface mannose receptors, a marker of alternatively activated macrophages (Mantovani et al., 2002), in both CD14+ monocytes and THP1 cells (Figures S5A and S5B). We next examined the effect in vivo by implanting the murine mammary carcinoma cells 4T1 that stably expressed WT Snail, Snail2R, or a control vector into the mammary fat pads of BALB/c mice (Figure 6E). The majority of the 4T1-Snail-formed tumors expressed higher levels of acetylated Snail than did the 4T1-control- or 4T1-Snail2R-formed tumors (Figure S5C). The expression of Snail in 4T1 cells mildly increased the tumor size/weight but significantly promoted metastasis compared with the 4T1-Snail2R/4T1-control (Figures 6F–6H). Microscopically, the 4T1-Snail-formed tumors had an increased infiltration by TAMs (Figure 6I) and microvascular density (Figure 6J). The infiltrated TAMs primarily expressed arginase-1 (Figure S5D), a marker of alternatively activated macrophages (Mantovani et al., 2002).

To confirm the critical role of TNF-α secretion by cancer cells in Snail-mediated tumor progression, we generated murine Snail-expressing LLC1 cells (LLC1-Snail) and knocked down TNF-α in LLC1-Snail cells (Figure 7A). We inoculated the cells into the subcutaneous area of $Tnf^{-/-}$ mice to prevent confounding effects from host TNF-α and observed the impact of TNF-α knockdown in Snail-mediated cancer progression and recruitment of TAMs (Figure 7B). The overexpression of Snail in LLC1 cells resulted in increased tumor growth and promoted metastasis (Figures 7C and 7D). LLC1-Snail-formed tumors had a higher infiltration of TAMs (Figure 7E) and microvascular density (Figure 7F), and the infiltrated TAMs were mostly arginase-1 positive (Figure S6). The knockdown of TNF-α in LLC1-Snail reduced tumorigenesis, metastasis, TAM recruitment, and angiogenesis (Figures 7C–7F; Figure S6).

(D) Quantitative real-time PCR for analyzing the expression of *ERCC1* and *IL8* in FaDu cells treated with the conditioned medium from FaDu-CDH or FaDu-Snail. mRNA, messenger RNA. Data represent means ± SEM. *$p < 0.05$; **$p < 0.01$.
(E) Schema for representing the strategy in mining candidate cytokine genes regulated by Snail. qRT-PCR, quantitative real-time PCR.
(F) Western blot of TNF-α, CCL2, and CCL5 in FaDu-CDH versus FaDu-Snail versus FaDu-Snail2R. The fold change of target proteins was shown.
(G) Schematic representation of the organization of the promoter of *TNFA*, *CCL2*, and *CCL5*, and the corresponding luciferase reporter constructs pXP2-TNFA, pGL-CCL2, and pGL-CCL5. TSS, transcriptional start site; E1, exon 1. The black bars indicate the E-boxes, which are the putative binding sites of Snail.
(H) Luciferase (Luc) reporter assays for analyzing the activity of the *TNFA*, *CCL2*, and *CCL5* promoter constructs in 293T cells cotransfected with EECBP or an empty vector (EV). β-gal, β-galactosidase. Data represent means ± SEM. *$p < 0.05$.
See also Figure S4 and Tables S1 and S2.

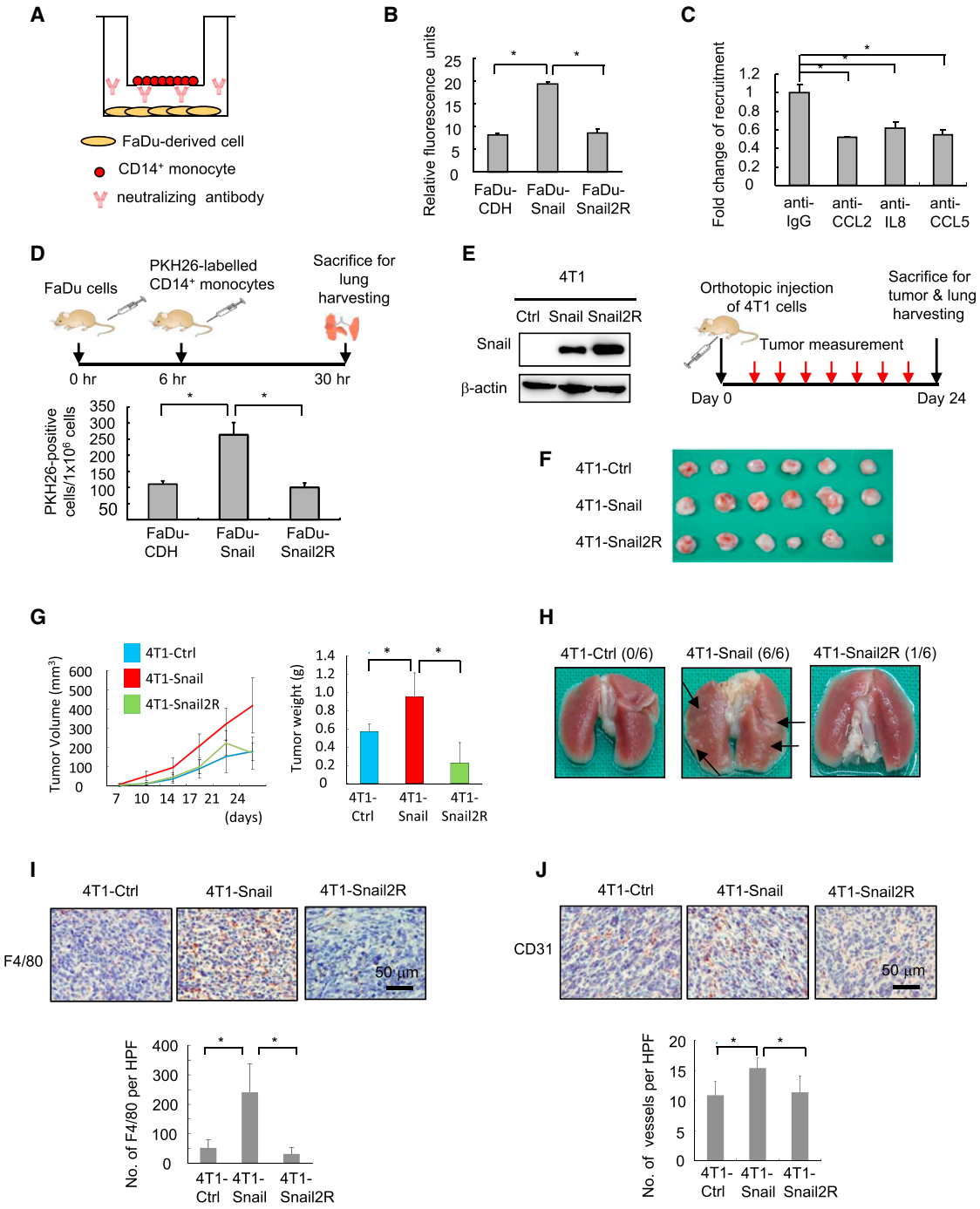

Figure 6. Snail Acetylation Promotes the Recruitment of TAMs and Tumor Progression

(A) Schema for representing the monocytes migration experiment.

(B) Transwell migration assay of human CD14$^+$ monocytes attracted by FaDu-CDH, FaDu-Snail, or FaDu-Snail2R. Data represent means ± SEM. *$p < 0.05$.

(C) Transwell migration assay of monocytes attracted by FaDu-Snail. Different neutralizing antibodies were added as indicated. Data represent means ± SEM. *$p < 0.05$. IgG, immunoglobulin G.

(D) In vivo macrophages rapid recruitments assay. Upper, schema for animal experiment; lower, quantification of the recruited PKH26-labeled macrophages in lungs of the mice 30 hr after monocytes injection. n = 5 for each group. Data represent means ± SEM. *$p < 0.05$.

(E–J) Orthotopic imaplantation assay. The 4T1 cells expressing WT Snail, nonacetylatable Snail (Snail2R), or a control vector were inoculated into the mammary fat pad of the BALB/c mice. The tumor volume was measured regularly, and the mice were sacrificed after 24 days. n = 6 for each group. (E) Left: western blot to confirm the expression of ectopic WT Snail and Snail2R in 4T1 cells. Right: schema of the experiment. (F) The photo of orthotopic tumors. (G) The tumor volume (left) and tumor weight (right) of orthotopic tumors. Data represent means ± SEM. *$p < 0.05$. (H) Representative photos of the lungs of mice implanted with indicated cells. The arrows indicate the metastatic tumors in lung. The numbers in the parentheses indicate the metastatic-tumor-forming mice/total mice in each

(legend continued on next page)

Snail Acetylation Is Associated with TAM Recruitment and Poor Prognosis of Head and Neck Cancer Patients

Finally, we confirmed the proposed mechanism in public array database and human cancer specimens. First, we investigated the correlation between *SNAI1* and the target genes in the public database. In array data from the NCI-60 panel, the level of *SNAI1* significantly correlated with the expression levels of *CCL2* and *CCL5,* while *SNAI1* was inversely correlated with *CDH1* (Figure S7A). In data obtained from ONCOMINE (Rhodes et al., 2004), the expression patterns of *SNAI1*, *CCL2*, and *CCL5* for head and neck cancers originating from different sites were similar (Figure S7B). Next, we confirmed the correlation and clinical significance of Snail acetylation and TAMs in human cancer specimens. A significant correlation between the percentage of acetylated Snail (detected by the PLA) and the number of TAMs was shown in tumor tissue samples from patients with head and neck cancers (Figures 8A and 8B; Table S3). The expression of acetylated Snail (detected by an anti-acetylated Snail Lys187 antibody) was correlated with increased infiltration of TAMs in head and neck cancers (Figure 8C; Table S4) and in lung cancers (Figure S7C). A concomitant increase in acetylated Snail and TAM numbers was correlated with a shorter progression-free survival in head and neck cancer patients (Figure 8D).

DISCUSSION

Several transcriptional factors have been known to function as both a repressor and an activator by associating with different coregulators, such as the nuclear receptors (McKenna and O'Malley, 2002) and the MEF2 family of transcriptional factors (McKinsey et al., 2002), which extends their functional flexibility. Lysine acetylation of the histone and nonhistone proteins plays a crucial role in regulating fundamental biological processes, including gene expression (Choudhary et al., 2009). A great example is the p53 acetylation in target gene regulation (Brooks and Gu, 2011). Here, we demonstrate that the acetylation of Snail affects its association with different coregulators, thereby determining it as an activator or a repressor. Interestingly, acetylated Snail can act either as an activator (e.g., in *ERCC1*) or as a coactivator (e.g., in *FN1*), which greatly extends the function of Snail during cancer metastasis. Another interesting question is whether Snail acetylation affects the EMT phenotype, given that acetylated Snail prohibits repressor complex formation. Our ChIP experiments showed that acetylated Snail binds to the promoters of activated target genes and that nonacetylated Snail binds to the promoters of repressed target genes simultaneously in the same cells. Furthermore, Snail also induces the expression of Zeb1, which is another major EMT inducer that directly represses E-cadherin expression. This finding may explain why cancer cells expressing acetylatable Snail are still capable of repressing E-cadherin. Here, we also found that Snail acetylation more prominently promotes tumor metastasis compared with primary tumor growth. The possible explanation is that Snail activation may induce cell cycle arrest (Vega et al., 2004; Hu et al., 2010), which could attenuate its impact on primary tumor growth.

In this study, we identified that TNF-α is the crucial exogenous stimulus for Snail acetylation and that TNF-α and Snail form a positive feedback loop to amplify the signal. The importance of TNF-α in triggering EMT of cancer cells has been shown in previous studies (Wu and Zhou, 2010). TNF-α induces EMT through the NFκB-mediated transcription of *TWIST1* (Li et al., 2012) and stabilizes Snail through CSN2 (Wu et al., 2009). Together with our current findings and those obtained in previous studies, we suggest that TNF-α has dual effects on Snail: TNF-α stabilizes Snail to increase its amount and promotes Snail acetylation to activate the transcription of target genes. However, although few studies have utilized etanercept, a decoy receptor of TNF-α, in cancer treatment (Wu et al., 2013), the overall benefit of blocking TNF-α is minimal (Zidi et al., 2010). In this study, we showed that etanercept abrogates acetylated Snail-induced target gene transcription and that IKKα is crucial for TNF-α-mediated Snail acetylation. Therefore, we suggest that understanding the activity of the TNF-α-IKKα-acetylated Snail pathway may improve the effectiveness of using etanercept in cancer treatment.

TAMs mainly have a phenotype resembling the alternatively activated M2 macrophages (Biswas and Mantovani, 2010). In this study, we show that the cancer cells expressing acetylated Snail not only recruit TAMs by secreting CCL2, CCL5, and IL8 but also induce macrophages to exhibit an M2-like phenotype (expressing the mannose receptor and promoting angiogenesis). However, the expression of cytokines for the M2 polarization of macrophages, e.g., interleukin 10 and interleukin 13, was not elevated in Snail-expressing cancer cells (Table S2). Whether these cancer cells induce an M2-like polarization through nonclassical M2-polarizing cytokines or through recruiting/activating of other immune cells, e.g., Th2 cells (Stein et al., 1992), is unknown and needs to be further addressed.

In conclusion, our study discovered that cancer cells containing acetylated Snail modulate the cytokinome in the tumor microenvironment. This finding extends the repertoire of roles for Snail. Therefore, we have contributed to a comprehensive understanding of Snail's functions in the metastatic process, including its role as a transcriptional activator for inducing cytokine expression in the tumor microenvironment and as a transcriptional repressor for suppressing adherent protein expression in driving cancer cell migration.

EXPERIMENTAL PROCEDURES

In Vitro Acetylation and Deacetylation Assay

The HAT domain of the p300/CBP protein was purchased from the Upstate Company (#14-418, Merck KGaA). The in vitro acetylation assay was performed using biotin-tagged peptides that contain a portion of Snail around lysine 146 (QLAQLSEAKDLQAR) or lysine 187 (VCGTCGKAFSRPW). Peptides in which lysine was replaced with the nonacetylatable aa arginine (QLAQL SEARDLQAR, VCGTCGRAFSRPW) were used as controls in the experiment. In the standard assay, 0.5 μg peptide, 0.5 μg of the HAT domain of the

group. (I) Upper: IHC of F4/80 for showing the recruitments of macrophages in orthotopic tumors. Scale bar, 50 μm. Lower: quantification of F4/80-positive cells per high power field (HPF). Data represent means ± SEM. *$p < 0.05$. (J) Upper: IHC of CD31 in orthotopic tumors. Scale bar, 50 μm. Lower: quantification of the vessels per HPF. Data represent means ± SEM. *$p < 0.05$.
See also Figure S5.

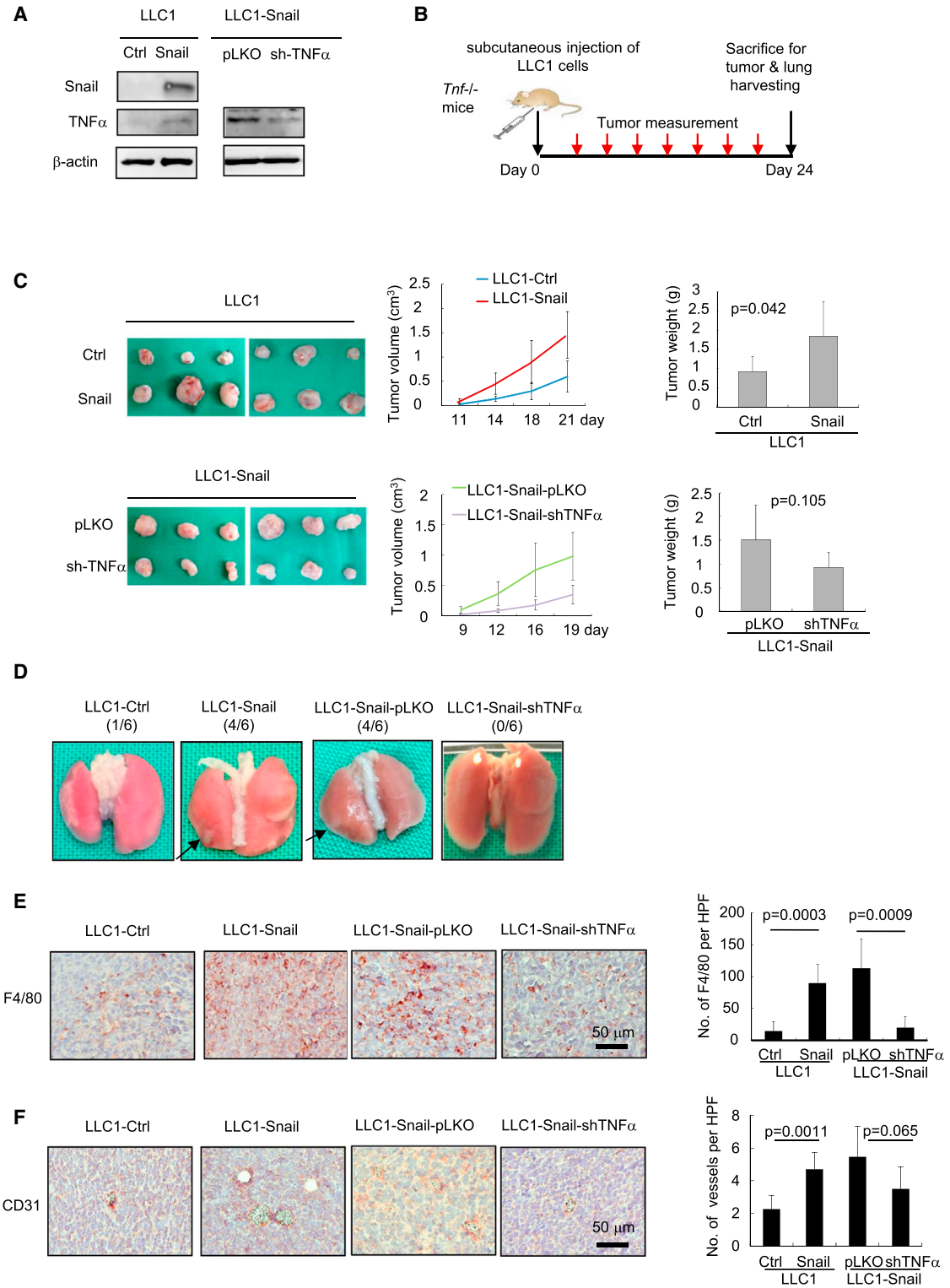

Figure 7. Tumor-Secreted TNF-α Is Critical for Snail-Induced Tumor Progression

(A) Western blot for confirming the expression of Snail and TNF-α in the LLC1 cells expressing WT murine Snail (LLC1-Snail) or a control vector (LLC1-Ctrl), and the LLC1-Snail cells receiving shRNA against murine TNF-α or a control vector (pLKO).

(B) Schema of the experiment. The LLC1 cells were inoculated into subcutaneous area of the *Tnf*$^{-/-}$ mice (n = 6 for each group). The tumor volume was measured regularly and the mice were sacrificed after 24 days.

(C) Left: photos of LLC1-formed tumors. Right: the tumor volume and tumor weight. Data represent means ± SEM. The p value is shown in each panel.

(legend continued on next page)

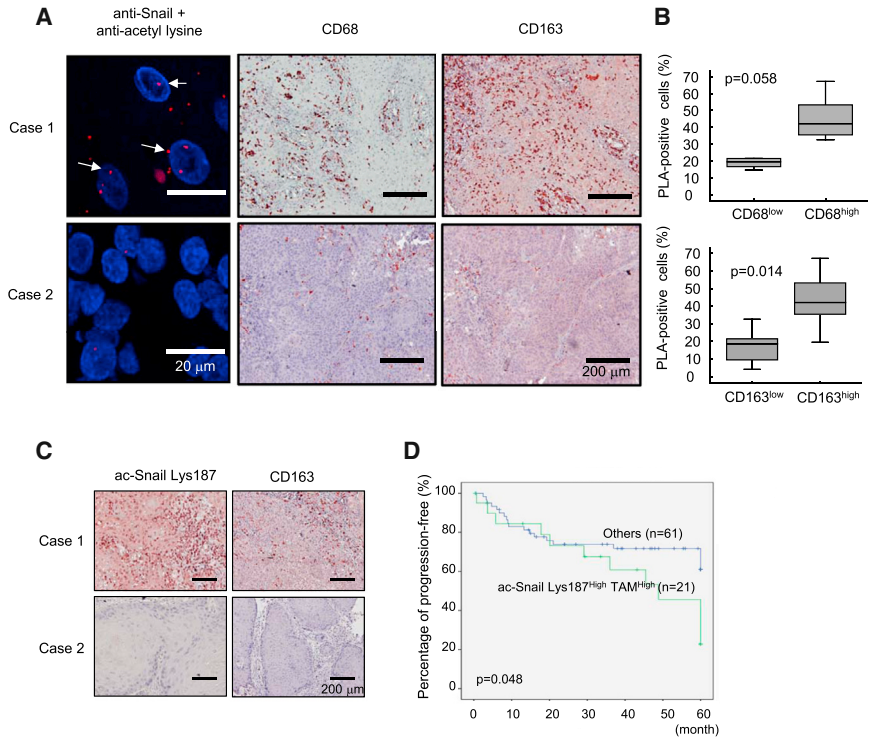

Figure 8. Clinical Significance of Snail Acetylation in Head and Neck Cancer Patients

(A) PLA for detecting acetylated Snail (left) and IHC for analyzing $CD68^+$ (middle) or $CD163^+$ (right) macrophages in head and neck cancer patients. The arrows indicate the representative PLA-positive signals. Case 1 is a representative case with increased acetylated Snail and $CD68^+/CD163^+$ macrophages. Case 2 is a representative case with low acetylated Snail and macrophage recruitments. Scale bars: for PLA photo, 20 μm; for CD68/CD163 IHC, 200 μm.

(B) The box plot for showing the percentage of PLA-positive cells in $CD68^{low}$ versus $CD68^{high}$ (upper panel) and $CD163^{low}$ versus $CD163^{high}$ (lower panel) head and neck cancer samples (n = 15). The p value was shown in each panel. The box plots represent sample maximum (upper end of whisker), upper quartile (top of box), median (band in the box), lower quartile (bottom of box), and sample minimum (lower end of whisker).

(C) Representative results of immunohistochemistry using the antibody against acetylated Snail lysine 187 or a macrophage marker CD163 in head and neck cancer samples. Case 1, a representative case of increased acetylated Snail in cancer cells and tumor-associated macrophages. Case 2, a representative case of low level of acetylated Snail in cancer cells and few macrophages. Scale bars, 200 μm.

(D) A Kaplan-Meier analysis of the progression-free survival in 82 head and neck cancer patients. The p value is shown in the panel.

See also Figure S7 and Tables S3 and S4.

p300/CBP protein, 1 μg acetyl-CoA (No. A2181, Sigma-Aldrich), and 4 μl 5× HAT assay buffer (250 mM Tris-HCl, pH 8.0, 50% glycerol, 0.5 mM EDTA, 5 mM dithiothreitol) were incubated for 30 min. The reaction products were loaded onto the nitrocellulose paper and blotted with an anti-acetyl-lysine antibody. The in vitro deacetylation assay was performed by incubating HDAC1, HDAC2, and HDAC3 (Nos. 31342, 31343, and 31349, respectively; Active Motif) with glutathione S-transferase (GST)-purified Snail from 293T cells co-transfected with pHA-CBP and pGST-Snail. In this assay, 0.25 or 0.5 μg HDAC and 0.5 μg GST-Snail were incubated with deacetylation buffer (10 mM Tris-HCl, pH 8.0, 100 mM NaCl) for 30 min. The reaction products were subjected to western blot analysis and detected using the anti-acetylated lysine 146 and lysine 187 Snail antibodies.

Animal Experiments

The animal experiments were approved by the Institutional Animal Care and Utilization Committee of Taipei Veterans General Hospital (case no. IACUC2013-038). The animal experiments include three parts. The first one is the in vivo macrophages recruitment assay. Human $CD14^+$ monocytes were incubated with 2 μM PKH26 for 5 min at room temperature, followed by the addition of an equal volume of serum to stop the reaction. Each nonobese diabetic-severe combined immunodeficiency mouse received an injection of 1×10^6 FaDu-CDH or FaDu-Snail or FaDu-Snail2R cells (n = 5 for each group). After 6 hr, 2×10^5 PKH26-labeled monocytes were injected into the tail veins of the same mice; then the mice were sacrificed, and the lungs were harvested 30 hr following the monocyte injection. The lungs were trypsinized with 0.25% trypsin and 2.5 mg/ml collagenase I for 45 min at 37°C. Every 5–8 min during this incubation, the tube was gently agitated for a few seconds. After 45 min of incubation, the tube was then vigorously shaken for 30 s to dissolve the lung, and the resulting tissue/cell suspension was filtered through a 70 μm strainer. The recruited macrophages were quantified by flow cytometry to detect PKH26-labeled cells. The second experiment is the orthotopic implantation assay. 4T1 cells expressing WT or mutant Snail or a control vector were injected into the mammary fat pad of BALB/c mice (n = 6 for each group). The size of the orthotopic tumors was measured regularly throughout the experiment. The mice were sacrificed 24 days after tumor inoculation, and the orthotopic tumors were harvested for measuring weight, TAM infiltrations, and microvascular densities (MVDs). The development of metastatic lung tumors was observed in each group. The third experiment is implanting LLC1 cells into $Tnf^{-/-}$ mice to observe the effect of tumor-secreted TNF-α on cancer metastasis. The $Tnf^{-/-}$ mice have previously been described (Pasparakis et al., 1996; Chio et al., 2012). For mouse typing, genomic DNA samples were prepared from tail tissues harvested from the mice and genotyped by PCR using specific primer sets. The LLC1 cells were stably transfected with murine Snail or a control vector, and the LLC1-Snail cells were transfected with a shRNA against *Tnf* or a control sequence. Then, the cells were inoculated into the subcutaneous area of mice (n = 6 for each group). The size of the tumors was measured regularly. The mice were sacrificed 24 days after tumor inoculation, and the tumors were harvested to measure the weight,

(D) Representative photos of the lungs of mice implanted with indicated cells. The arrows indicate the metastatic tumors in lungs. The numbers in the parentheses indicate the metastatic-tumor-forming mice/total mice in each group.

(E) Left: IHC of F4/80 for showing the recruitments of macrophages in LLC1-formed tumors. Scale bar, 50 μm. Right: quantification of F4/80-positive cells per high power field (HPF). Data represent means ± SEM. The p value is shown in the corresponding panels.

(F) Left: IHC of CD31 in LLC1-formed tumors. Scale bar, 50 μm. Right: quantification of the vessels per HPF. Data represent means ± SEM. The p value is shown in each panel.

See also Figure S6.

TAMs infiltration, and MVDs. The development of metastatic lung tumors was observed in each group.

Patient Samples

This study was approved by the Institutional Review Board of Taipei Veterans General Hospital (case no. VGHIRB-2013-04-035B), and the informed consents have been obtained from all patients. We used three sets of samples to investigate the correlation between acetylated Snail and TAM infiltration. The first group, which contained 15 paraffin-embedded head and neck cancer samples from patients receiving treatment at the Department of Otolaryngology of Taipei Veterans General Hospital, was used for the PLA and CD163 staining. The characteristics of the 15 patients are listed in Table S3, and the results are shown in Figures 7A and 7B. The second group contained samples from 82 head and neck cancer patients, and the samples were used for immunohistochemistry (IHC) using the antibody against acetylated Snail lysine 187 and CD163. The characteristics of the 82 patients are listed in Table S4, and the results are shown in Figures 7C and 7D. The third group included ten non-small-cell lung cancer samples. A representative IHC result is shown in Figure S6C.

Statistical Analysis

A two-tailed independent Student's t test was used to compare the continuous variables between the two groups. The chi-square test was applied to compare dichotomous variables. The Kaplan-Meier estimation and the log-rank test were used to compare survival between the patient groups. All the statistical data were derived from at least two biological independent experiments, and each experiment contained two technical replicates. The level of statistical significance was set at $p \nleq 0.05$ for all tests.

ACCESSION NUMBERS

The data sets of the cDNA microarray for FaDu-CDH versus FaDu-Snail and FaDu-Snail2R were deposited at Gene Expression Omnibus with the accession number GSE58592.

SUPPLEMENTAL INFORMATION

Supplemental Information includes Supplemental Experimental Procedures, seven figures, and four tables and can be found with this article online at http://dx.doi.org/10.1016/j.ccell.2014.09.002.

AUTHOR CONTRIBUTIONS

M.-H.Y. and D.S.-S.H. conceived and designed the experiments. D.S.-S.H., H.-J.W., C.-H.C., C.-H.H., and P.-H.C. performed the experiments, with the help of N.-J.C. on animal experiments. D.S.-S.H., H.-J.W., and M.-H.Y. analyzed the data. M.-H.Y. and D.S.-S.H. wrote the paper. S.-K.T. provided the head and neck cancer samples and clinical information.

ACKNOWLEDGMENTS

We thank Dr. Mien-Chie Hung (University of Texas M.D. Anderson Cancer Center) for the invaluable comments on the manuscript and generous gifts of the pFLAG-CBP, pHA-CBP, pHA-EECBP, pHA-AACBP, and Snail6SA plasmids, and IKK$\alpha^{-/-}$, IKK$\beta^{-/-}$, IKK$\gamma^{-/-}$ MEFs. We thank Drs. Fung-Fang Wang, Kou-Juey Wu, Kuang-Hui Sun, and Teh-Ying Chou (all from National Yang-Ming University) for the pRC-CMV-p53 plasmid, pMT2T-p65 plasmid, LLC1 cell line, and the lung cancer samples, respectively. We thank Dr. Pan-Chyr Yang (National Taiwan University) for the CL1-1 and CL1-5 cell lines. We thank the Instrument Center of National Chung-Hsing University for technical support of the mass spectrometry analysis. This work was supported by the National Health Research Institutes (NHRI-EX103-10331BI to M-H.Y.); the Ministry of Science and Technology (102-2321-B-010-006 and 103-2321-B-010-019 to M.-H.Y.; 101-2314-B-010-021-MY3 to S.-K.T.); Taipei Veterans General Hospital (V103-E8-002 to M.-H.Y.); Veterans General Hospitals-University System of Taiwan Joint Research Program (VGHUST103-G-7-5-1 to M.-H.Y.); a grant from Ministry of Education, Aim for the Top University Plan (to M.-H.Y and N.-J.C.); and a grant from the Ministry of Health and Welfare, Center of Excellence for Cancer Research (MOHW103-TD-B-111-02 to M.-H.Y.).

Received: March 11, 2014
Revised: July 18, 2014
Accepted: September 16, 2014
Published: October 13, 2014

REFERENCES

Ansieau, S., Bastid, J., Doreau, A., Morel, A.P., Bouchet, B.P., Thomas, C., Fauvet, F., Puisieux, I., Doglioni, C., Piccinin, S., et al. (2008). Induction of EMT by twist proteins as a collateral effect of tumor-promoting inactivation of premature senescence. Cancer Cell *14*, 79–89.

Azenshtein, E., Luboshits, G., Shina, S., Neumark, E., Shahbazian, D., Weil, M., Wigler, N., Keydar, I., and Ben-Baruch, A. (2002). The CC chemokine RANTES in breast carcinoma progression: regulation of expression and potential mechanisms of promalignant activity. Cancer Res. *62*, 1093–1102.

Berger, S.L. (2007). The complex language of chromatin regulation during transcription. Nature *447*, 407–412.

Biswas, S.K., and Mantovani, A. (2010). Macrophage plasticity and interaction with lymphocyte subsets: cancer as a paradigm. Nat. Immunol. *11*, 889–896.

Brooks, C.L., and Gu, W. (2011). The impact of acetylation and deacetylation on the p53 pathway. Protein Cell *2*, 456–462.

Cano, A., Pérez-Moreno, M.A., Rodrigo, I., Locascio, A., Blanco, M.J., del Barrio, M.G., Portillo, F., and Nieto, M.A. (2000). The transcription factor snail controls epithelial-mesenchymal transitions by repressing E-cadherin expression. Nat. Cell Biol. *2*, 76–83.

Chio, I.I., Sasaki, M., Ghazarian, D., Moreno, J., Done, S., Ueda, T., Inoue, S., Chang, Y.L., Chen, N.J., and Mak, T.W. (2012). TRADD contributes to tumour suppression by regulating ULF-dependent p19Arf ubiquitylation. Nat. Cell Biol. *14*, 625–633.

Choudhary, C., Kumar, C., Gnad, F., Nielsen, M.L., Rehman, M., Walther, T.C., Olsen, J.V., and Mann, M. (2009). Lysine acetylation targets protein complexes and co-regulates major cellular functions. Science *325*, 834–840.

De Craene, B., and Berx, G. (2013). Regulatory networks defining EMT during cancer initiation and progression. Nat. Rev. Cancer *13*, 97–110.

Eckert, M.A., Lwin, T.M., Chang, A.T., Kim, J., Danis, E., Ohno-Machado, L., and Yang, J. (2011). Twist1-induced invadopodia formation promotes tumor metastasis. Cancer Cell *19*, 372–386.

Goldfeld, A.E., Doyle, C., and Maniatis, T. (1990). Human tumor necrosis factor alpha gene regulation by virus and lipopolysaccharide. Proc. Natl. Acad. Sci. USA *87*, 9769–9773.

Gu, W., and Roeder, R.G. (1997). Activation of p53 sequence-specific DNA binding by acetylation of the p53 C-terminal domain. Cell *90*, 595–606.

Guo, Y., Xu, F., Lu, T., Duan, Z., and Zhang, Z. (2012). Interleukin-6 signaling pathway in targeted therapy for cancer. Cancer Treat. Rev. *38*, 904–910.

Guttridge, D.C., Albanese, C., Reuther, J.Y., Pestell, R.G., and Baldwin, A.S., Jr. (1999). NF-kappaB controls cell growth and differentiation through transcriptional regulation of cyclin D1. Mol. Cell. Biol. *19*, 5785–5799.

Herranz, N., Pasini, D., Díaz, V.M., Francí, C., Gutierrez, A., Dave, N., Escrivà, M., Hernandez-Muñoz, I., Di Croce, L., Helin, K., et al. (2008). Polycomb complex 2 is required for E-cadherin repression by the Snail1 transcription factor. Mol. Cell. Biol. *28*, 4772–4781.

Hou, Z., Peng, H., Ayyanathan, K., Yan, K.P., Langer, E.M., Longmore, G.D., and Rauscher, F.J., 3rd. (2008). The LIM protein AJUBA recruits protein arginine methyltransferase 5 to mediate SNAIL-dependent transcriptional repression. Mol. Cell. Biol. *28*, 3198–3207.

Hsu, D.S., Lan, H.Y., Huang, C.H., Tai, S.K., Chang, S.Y., Tsai, T.L., Chang, C.C., Tzeng, C.H., Wu, K.J., Kao, J.Y., and Yang, M.H. (2010). Regulation of excision repair cross-complementation group 1 by Snail contributes to cisplatin resistance in head and neck cancer. Clin. Cancer Res. *16*, 4561–4571.

Hu, C.T., Chang, T.Y., Cheng, C.C., Liu, C.S., Wu, J.R., Li, M.C., and Wu, W.S. (2010). Snail associates with EGR-1 and SP-1 to upregulate transcriptional activation of p15INK4b. FEBS J. *277*, 1202–1218.

Huang, W.C., Ju, T.K., Hung, M.C., and Chen, C.C. (2007). Phosphorylation of CBP by IKKalpha promotes cell growth by switching the binding preference of CBP from p53 to NF-kappaB. Mol. Cell *26*, 75–87.

Hwang, W.L., Yang, M.H., Tsai, M.L., Lan, H.Y., Su, S.H., Chang, S.C., Teng, H.W., Yang, S.H., Lan, Y.T., Chiou, S.H., et al. (2011). The Snail-IL8 axis engenders stemness and tumorigenic characteristics in human colorectal carcinoma. Gastroenterology *141*, 279–291.

Hwang, W.L., Jiang, J.K., Yang, S.H., Huang, T.S., Lan, H.Y., Teng, H.W., Yang, C.Y., Tsai, Y.P., Lin, C.H., Wang, H.W., and Yang, M.H. (2014). MicroRNA-146a directs the symmetric division of Snail-dominant colorectal cancer stem cells. Nat. Cell Biol. *16*, 268–280.

Ito, A., Lai, C.H., Zhao, X., Saito, S., Hamilton, M.H., Appella, E., and Yao, T.P. (2001). p300/CBP-mediated p53 acetylation is commonly induced by p53-activating agents and inhibited by MDM2. EMBO J. *20*, 1331–1340.

Javaid, S., Zhang, J., Anderssen, E., Black, J.C., Wittner, B.S., Tajima, K., Ting, D.T., Smolen, G.A., Zubrowski, M., Desai, R., et al. (2013). Dynamic chromatin modification sustains epithelial-mesenchymal transition following inducible expression of Snail-1. Cell Reports *5*, 1679–1689.

Li, C.W., Xia, W., Huo, L., Lim, S.O., Wu, Y., Hsu, J.L., Chao, C.H., Yamaguchi, H., Yang, N.K., Ding, Q., et al. (2012). Epithelial-mesenchymal transition induced by TNF-α requires NF-κB-mediated transcriptional upregulation of Twist1. Cancer Res. *72*, 1290–1300.

Loetscher, P., Seitz, M., Clark-Lewis, I., Baggiolini, M., and Moser, B. (1994). Both interleukin-8 receptors independently mediate chemotaxis. Jurkat cells transfected with IL-8R1 or IL-8R2 migrate in response to IL-8, GRO alpha and NAP-2. FEBS Lett. *341*, 187–192.

Lyons, J.G., Patel, V., Roue, N.C., Fok, S.Y., Soon, L.L., Halliday, G.M., and Gutkind, J.S. (2008). Snail up-regulates proinflammatory mediators and inhibits differentiation in oral keratinocytes. Cancer Res. *68*, 4525–4530.

Mani, S.A., Guo, W., Liao, M.J., Eaton, E.N., Ayyanan, A., Zhou, A.Y., Brooks, M., Reinhard, F., Zhang, C.C., Shipitsin, M., et al. (2008). The epithelial-mesenchymal transition generates cells with properties of stem cells. Cell *133*, 704–715.

Mantovani, A., Sozzani, S., Locati, M., Allavena, P., and Sica, A. (2002). Macrophage polarization: tumor-associated macrophages as a paradigm for polarized M2 mononuclear phagocytes. Trends Immunol. *23*, 549–555.

McKenna, N.J., and O'Malley, B.W. (2002). Combinatorial control of gene expression by nuclear receptors and coregulators. Cell *108*, 465–474.

McKinsey, T.A., Zhang, C.L., and Olson, E.N. (2002). MEF2: a calcium-dependent regulator of cell division, differentiation and death. Trends Biochem. Sci. *27*, 40–47.

Pasparakis, M., Alexopoulou, L., Episkopou, V., and Kollias, G. (1996). Immune and inflammatory responses in TNF alpha-deficient mice: a critical requirement for TNF alpha in the formation of primary B cell follicles, follicular dendritic cell networks and germinal centers, and in the maturation of the humoral immune response. J. Exp. Med. *184*, 1397–1411.

Peinado, H., Ballestar, E., Esteller, M., and Cano, A. (2004). Snail mediates E-cadherin repression by the recruitment of the Sin3A/histone deacetylase 1 (HDAC1)/HDAC2 complex. Mol. Cell. Biol. *24*, 306–319.

Qian, B.Z., Li, J., Zhang, H., Kitamura, T., Zhang, J., Campion, L.R., Kaiser, E.A., Snyder, L.A., and Pollard, J.W. (2011). CCL2 recruits inflammatory monocytes to facilitate breast-tumour metastasis. Nature *475*, 222–225.

Rembold, M., Ciglar, L., Yáñez-Cuna, J.O., Zinzen, R.P., Girardot, C., Jain, A., Welte, M.A., Stark, A., Leptin, M., and Furlong, E.E. (2014). A conserved role for Snail as a potentiator of active transcription. Genes Dev. *28*, 167–181.

Rhodes, D.R., Yu, J., Shanker, K., Deshpande, N., Varambally, R., Ghosh, D., Barrette, T., Pandey, A., and Chinnaiyan, A.M. (2004). ONCOMINE: a cancer microarray database and integrated data-mining platform. Neoplasia *6*, 1–6.

Stanisavljevic, J., Porta-de-la-Riva, M., Batlle, R., de Herreros, A.G., and Baulida, J. (2011). The p65 subunit of NF-κB and PARP1 assist Snail1 in activating fibronectin transcription. J. Cell Sci. *124*, 4161–4171.

Stein, M., Keshav, S., Harris, N., and Gordon, S. (1992). Interleukin 4 potently enhances murine macrophage mannose receptor activity: a marker of alternative immunologic macrophage activation. J. Exp. Med. *176*, 287–292.

Ueda, A., Ishigatsubo, Y., Okubo, T., and Yoshimura, T. (1997). Transcriptional regulation of the human monocyte chemoattractant protein-1 gene. Cooperation of two NF-kappaB sites and NF-kappaB/Rel subunit specificity. J. Biol. Chem. *272*, 31092–31099.

Vega, S., Morales, A.V., Ocaña, O.H., Valdés, F., Fabregat, I., and Nieto, M.A. (2004). Snail blocks the cell cycle and confers resistance to cell death. Genes Dev. *18*, 1131–1143.

Wickremasinghe, M.I., Thomas, L.H., O'Kane, C.M., Uddin, J., and Friedland, J.S. (2004). Transcriptional mechanisms regulating alveolar epithelial cell-specific CCL5 secretion in pulmonary tuberculosis. J. Biol. Chem. *279*, 27199–27210.

Wu, Y., and Zhou, B.P. (2010). TNF-alpha/NF-kappaB/Snail pathway in cancer cell migration and invasion. Br. J. Cancer *102*, 639–644.

Wu, Y., Deng, J., Rychahou, P.G., Qiu, S., Evers, B.M., and Zhou, B.P. (2009). Stabilization of snail by NF-kappaB is required for inflammation-induced cell migration and invasion. Cancer Cell *15*, 416–428.

Wu, M.Z., Tsai, Y.P., Yang, M.H., Huang, C.H., Chang, S.Y., Chang, C.C., Teng, S.C., and Wu, K.J. (2011). Interplay between HDAC3 and WDR5 is essential for hypoxia-induced epithelial-mesenchymal transition. Mol. Cell *43*, 811–822.

Wu, C., Fernandez, S.A., Criswell, T., Chidiac, T.A., Guttridge, D., Villalona-Calero, M., and Bekaii-Saab, T.S. (2013). Disrupting cytokine signaling in pancreatic cancer: a phase I/II study of etanercept in combination with gemcitabine in patients with advanced disease. Pancreas *42*, 813–818.

Yang, W.H., Lan, H.Y., Huang, C.H., Tai, S.K., Tzeng, C.H., Kao, S.Y., Wu, K.J., Hung, M.C., and Yang, M.H. (2012). RAC1 activation mediates Twist1-induced cancer cell migration. Nat. Cell Biol. *14*, 366–374.

Zhou, B.P., Deng, J., Xia, W., Xu, J., Li, Y.M., Gunduz, M., and Hung, M.C. (2004). Dual regulation of Snail by GSK-3beta-mediated phosphorylation in control of epithelial-mesenchymal transition. Nat. Cell Biol. *6*, 931–940.

Zidi, I., Mestiri, S., Bartegi, A., and Amor, N.B. (2010). TNF-alpha and its inhibitors in cancer. Med. Oncol. *27*, 185–198.